A Mathematical Model for the Flash Calcination of Dispersed CaCO3 and Ca(OH)2 Particles

ARTICLE *in* INDUSTRIAL & ENGINEERING CHEMISTRY RESEARCH · FEBRUARY 1989

Impact Factor: 2.59 · DOI: 10.1021/ie00086a005

3 AUTHORS, INCLUDING:

Geoffrey D. Silcox
University of Utah
66 PUBLICATIONS **748** CITATIONS
SEE PROFILE

John C. Kramlich
University of Washington Seattle
98 PUBLICATIONS **1,232** CITATIONS
SEE PROFILE

A Mathematical Model for the Flash Calcination of Dispersed $CaCO_3$ and $Ca(OH)_2$ Particles

Geoffrey D. Silcox,* John C. Kramlich, and David W. Pershing
Energy and Environmental Research Corporation, 18 Mason, Irvine, California 92718

A mathematical model for the flash calcination of $Ca(OH)_2$ and $CaCO_3$ is presented. The model describes the decomposition of the parent material at the reactant–product interface, the diffusion of CO_2 or H_2O through the growing CaO layer, and the sintering of the CaO layer. The model is qualitative, but it provides useful estimates of peak CO_2 pressures in the CaO layer, relative rates of surface area development and loss for $Ca(OH)_2$ and $CaCO_3$, the effect of particle size, and the effects of time and temperature.

The emission of sulfur oxides (SO_2 and SO_3) from the combustion of high-sulfur coals in industrial boilers is generally viewed as a major contributor to acid rain. Consequently, there is considerable interest in the development of SO_2 control technologies, particularly if they are suitable for retrofit applications. One such technology involves the injection of dry, calcium-based sorbents into existing, coal-fired boilers. This approach involves the rapid heating and decomposition of $Ca(OH)_2$ or $CaCO_3$ to form CaO:

$$Ca(OH)_2 = CaO + H_2O$$

$$CaCO_3 = CaO + CO_2$$

The CaO formed in the calcination process is porous with a void fraction of about 0.5. Surface areas (BET with N_2) of flash-calcined limestone particles have been measured by Borgwardt (1985). They range from 50 to 60 m^2/g for calcination using nitrogen carrier gas in a flow reactor. The development of such high surface areas is important if CaO is to be effective at removing sulfur oxides from combustion gases.

In addition to performing flash calcination studies in a flow reactor, Borgwardt calcined 1-μm limestone particles in a differential reactor with pure N_2. He obtained surface areas as high as 90 m^2/g at 873 K. Powell and Searcy (1982) decomposed large $CaCO_3$ crystals in vacuum and measured surface areas that range from 130 m^2/g at 923 K to 60 m^2/g at 1173 K. They found that the surface areas were not significantly reduced by annealing at 1173 K in vacuum.

Beruto and Searcy (1976) observed the existence of an intermediate layer of CaO between the undercomposed $CaCO_3$ and the final CaO product which they believed to be a metastable form of CaO. Powell and Searcy (1982) demonstrated that this layer is actually a porous aggregate of small crystals of normal NaCl-type CaO which rearranges when its thickness reaches 10–50 μm. This is a strain-relieving process which yields the final CaO product. Powell and Searcy observed that the intermediate layer has a uniform pore size while the final product does not. A repacking of the small crystals is responsible for the development of the distribution of pore sizes.

Further indications of the dynamic nature of the calcination process are reported by Borgwardt et al. (1986). They found that the surface areas of calcined, 1-μm $CaCO_3$ particles were strongly dependent on the sintering process to which they were subjected. Higher surface areas resulted from sintering in an inert sweep gas. Lower values resulted from stagnant conditions or from sintering with a sweep gas containing CO_2.

In summary, the flash calcination of dispersed limestone or $Ca(OH)_2$ particles produces CaO particles whose BET surface areas are dependent on the following: gas pressure, temperature, duration of exposure, CO_2 concentration, and possibly sorbent type. Anderson and Morgan (1964) and Anderson et al. (1965) report that the presence of moisture greatly accelerates the rate of sintering of MgO and CaO.

From the above discussion, it is clear that a mathematical model of the calcination and sintering process should include the following phenomena: decomposition of $CaCO_3$ at the $CaCO_3$–CaO interface, diffusion of the resulting CO_2 through the CaO layer, and sintering of the CaO layer. The sintering and decomposition steps are not understood fundamentally. The rate of calcination of $CaCO_3$ particles is known, however, from the work of Borgwardt (1985). Reliable data on the rate of sintering as a function of H_2O and CO_2 concentrations and of temperature do not currently exist. For these reasons, the model described below is qualitative but is still capable of providing useful estimates of the following: peak CO_2 pressures at the CaO–$CaCO_3$ interface, relative rates of surface area development and loss for $Ca(OH)_2$ and $CaCO_3$, the effect of particle size, and the effect of time and temperature.

Description of Model

The correlative, mathematical model outlined here describes the calcination and subsequent surface area loss of $CaCO_3$ and $Ca(OH)_2$ particles. The model parameters are based on the data of Borgwardt (1985) and Borgwardt et al. (1986). Although the results presented are primarily in terms of carbonate decomposition, all kinetic and transport equations are directly applicable to hydrates by appropriate adjustment of physical and chemical parameters. Comparison of hydrate and carbonate predictions are presented below.

The following steps are included in the model: decomposition of $CaCO_3$ at the CaO–$CaCO_3$ interface, diffusion of CO_2 through the CaO to the particle surface, diffusion of CO_2 from the particle surface to the bulk gas, and continuous surface area loss for all calcined material.

The overall concept for the model is shown in Figure 1. The calcination process is described by a shrinking core model for a spherical particle. For massive samples of $CaCO_3$, heat transfer may limit decomposition rates (Campbell et al., 1970), but for small, dispersed particles the rates of heat and mass transfer are not rate limiting (Powell and Searcy, 1982; Borgwardt, 1985). For this reason, the particle is assumed to be isothermal. As suggested by Figure 1, a CO_2 concentration gradient exists across the CaO layer. The calcination process is allowed to occur in steps leading to a layered CaO zone. Each layer

* Present address: Department of Chemical Engineering, University of Utah, Salt Lake City, UT 84112.

0888-5885/89/2628-0155$01.50/0

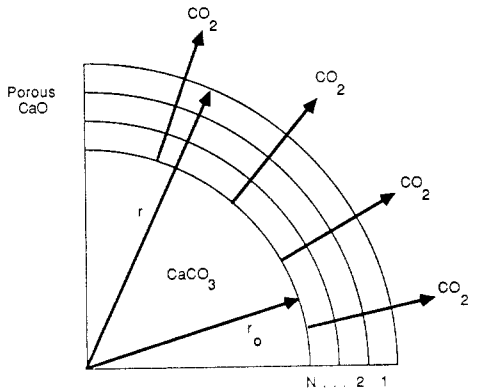

Figure 1. Schematic diagram of the calcination model. The particle is assumed to be spherical.

is homogeneous, and the physical properties within a given layer are constant. Physical properties are allowed to vary from layer to layer, with the most recently formed layer of CaO possessing the highest surface area. The rate of surface area loss is a function of temperature, surface area, and CO_2 concentration.

The equations governing the movement of the calcination front are

$$\frac{dr}{dt} = -\frac{M}{\rho}R_D \quad (\text{in m s}^{-1}) \tag{1}$$

and at $t = 0$,

$$r = r_o \tag{2}$$

where

$$R_D = k_D(P_e - P) \quad (\text{in kmol m}^{-2}\text{ s}^{-1})$$

$$k_D = 0.00122 \exp(-4026/T) \quad (\text{in kmol m}^{-2}\text{ s}^{-1}\text{ atm}^{-1})$$

$$P_e = \exp(17.74 - 0.00108T + 0.332 \ln T - 22020/T) \text{ (in atm)} \tag{3}$$

and r is the radius of the shrinking core of $CaCO_3$, t is time, M is the molecular weight of $CaCO_3$, ρ is the density (in kg m^{-3}) of $CaCO_3$, R_D is the rate of decomposition, r_o is the initial particle radius, which is assumed constant, k_D is a rate constant, P_e is the equilibrium dissociation pressure of CO_2 (in atm) (Weast, 1975), P is the CO_2 partial pressure at the CaO–$CaCO_3$ interface, and T is the absolute temperature (in K). Note that the rate of decomposition, R_D, approaches zero as P approaches P_e. This provides a means of allowing the decomposition reaction to slow itself should diffusion impede the escape of generated CO_2.

Several investigators, including Darroudi and Searcy (1981) and Hyatt et al. (1958), examined the effects of CO_2 pressure on decomposition kinetics; however, no one has yet developed an expression which is capable of explaining all of the data. The mechanism of decomposition is unknown. The CO_2 pressure dependence of eq 3 is consistent with the theory of Searcy and Beruto (1978) in which the rate-limiting step is solid-state diffusion of CO_2 or possibly a surface step for CO_2.

The diffusion of gaseous CO_2 in porous lime was studied by Campbell et al. (1970), who showed that the process is controlled by Knudsen diffusion. As part of the present study, the relative importance of ordinary diffusion, Knudsen diffusion, and hydrodynamic flow was examined. Knudsen diffusion is the controlling transport mechanism for CO_2 in porous lime; however, for moderately sintered CaO in which pore diameters are larger, ordinary diffusion becomes more important. For this reason, the diffusion coefficient is estimated as

$$D = (D_K^{-1} + D_{AB}^{-1})^{-1} \quad (\text{in m}^2\text{ s}^{-1}) \tag{4}$$

where

$$D_K = 0.00881T^{1/2}S^{-1} \quad (\text{in m}^2\text{ s}^{-1}) \tag{5}$$

and

$$D_{AB} = 0.000139(T/273)^{1.75}P_t^{-1} \quad (\text{in m}^2\text{ s}^{-1}) \tag{6}$$

Finally, the effective diffusivity for the porous material is estimated by

$$D_{eff} = D\epsilon^2 \tag{7}$$

where ϵ is the porosity of the calcine. Equation 7 approximates the calcine's tortuosity as ϵ^{-1}. Smith (1981) justifies the use of eq 7 by an application of the random pore model. In the above equations, D is the diffusion coefficient for the pore, D_K is the Knudsen diffusion coefficient, D_{AB} is the molecular diffusion coefficient for CO_2 in air, T is temperature (in K), S is the BET surface area (in m^2 kg^{-1}), and P_t is the total pressure (in atm).

The differential equation governing the diffusion of CO_2 through the porous lime is

$$\frac{\partial^2 P}{\partial R^2} + \left(\frac{2}{R} + \frac{1}{D_e}\frac{\partial D_e}{\partial R}\right)\frac{\partial P}{\partial R} = \frac{1}{D_e}\frac{\partial P}{\partial t} \tag{8}$$

with two boundary conditions:

at $R = r_o$

$$-D_e\frac{\partial P}{\partial R} = k_f(P - P_b) \tag{9}$$

at $R = r$

$$-\frac{D_e}{R_gT}\frac{\partial P}{\partial R} = k_D(P_e - P) \tag{10}$$

where R is the radial position within the calcined layer, k_f is the mass-transfer coefficient for a spherical particle, P_b is the CO_2 partial pressure in the bulk gas, and R_g is the gas constant. Equation 8 can be simplified by applying the pseudo-steady-state approximation for gas–solid reactions as described by Luss (1968). Furthermore, if each shell of calcine is assumed to be homogeneous, then for a given layer, D_e is constant. Equation 8 simplifies to

$$\frac{d^2P}{dR^2} + \frac{2}{R}\frac{dP}{dR} = 0 \tag{11}$$

The use of the pseudo-steady-state approximation is based on two observations: the calcination reaction is a gas–solid reaction and the predicted CO_2 pressures, at conditions of practical interest, are not sufficiently high to warrant abandoning the approximation.

Equation 11 applies to each shell of calcine. The shells or nodes are numbered as illustrated in Figure 1. The problem defined by eq 9–11 is analogous to a spherical, composite wall heat conduction problem. The positions of the nodes are defined by eq 1, which for sufficiently short time steps can be used to calculate r as a function of time:

$$r(t + \Delta t) = r(t) + \left.\frac{dr}{dt}\right|_t \Delta t \tag{12}$$

There is a CO_2 generation term at the $CaCO_3$–CaO interface (eq 10) and a convective boundary condition at the outer surface (eq 9). The solution to eq 9–11 is

for node 1

$$P_1 = P_b + \frac{R_N^2 k_D R_g T}{R_1^2 k_f}(P_e - P_N) \tag{13}$$

for nodes 2 through $N-1$

$$P_i = P_{i-1} + \frac{FR_gT}{4\pi(D_e)_{i-1}}\left(\frac{1}{R_i} - \frac{1}{R_{i-1}}\right) \quad (14)$$

where

$$F = 4\pi R_N^2 k_D(P_e - P_N)$$

for node N

$$P_N = \frac{P_e + BP_b}{1 + B} \quad (15)$$

where

$$B = \frac{A_1U_1}{4\pi R_N^2 k_D}$$

$$A_1 = \frac{4\pi R_1^2}{R_gT}$$

$$\frac{1}{U_1} = R_1^2\sum_{j=1}^{N-1}\frac{1}{(D_e)_j}\left(\frac{1}{R_{j+1}} - \frac{1}{R_j}\right) + \frac{1}{k_f}$$

The number of nodes increases by one with each step in time. Because the rate of calcination is a function of CO_2 partial pressure, eq 9–12 are all coupled. The layers of CaO are allowed to sinter at each time step which changes their transport properties. The rate of sintering is also a function of CO_2 partial pressure.

Surface Area Loss

In a series of differential reactor studies, Borgwardt et al. (1986) have shown that the rate of surface area loss is strongly dependent on time, temperature, nitrogen sweep rate, and CO_2 partial pressure. Because the sintering process for CaO is not understood fundamentally, an empirical approach to modeling is adopted here.

The surface area loss results of Borgwardt et al. are characterized by a rapid initial rate of loss followed by a slower rate of loss. At long times (about 5 min at 1273 K), the surface areas approach asymptotic values which are functions of temperature. At temperatures of practical importance for sulfation, 1200 K or greater, the asymptote is roughly 5 m^2/g. All calculations presented here assume an asymptotic value of 5 m^2/g.

Borgwardt et al.'s data can be described by the equation

$$dS/dt = -k(S - S_{as})^2 \quad (\text{in } m^2\ kg^{-1}\ s^{-1}) \quad (16)$$

where S is the BET surface area, t is time, k is a rate constant, and S_{as} is the asymptotic surface area. To account for the acceleration of sintering by CO_2, the rate constant (k) can be modified such that the activation energy decreases with increasing CO_2 partial pressure. One means of doing so involves expressing k as follows:

$$k = A\exp\left(-\frac{E}{R_gT}\right)\exp\left(\frac{BP^m}{R_gT}\right) \quad (\text{in kg m}^{-2}\ \text{s}^{-1}) \quad (17)$$

where A is a preexponential factor, E is an activation energy, P is the CO_2 partial pressure (in atm), m is a dimensionless exponent, and B is a constant. The second exponential on the right in eq 17 has the effect of lowering the activation energy for the sintering process. Based on data from Borgwardt et al. (1986), values of −0.111 and −314 atm m^3 k mol^{-1} are estimated for m and B, respectively. The activation energy (E) and the preexponential factor (A) are determined from the data of Borgwardt (1984) which are shown in Figure 2. The data of Figure 2 are qualitative. The precalcined material was not fully calcined so that some CO_2 may have been generated during the sintering process. In estimating values for A and E, a CO_2 concentration of 5000 ppm was assumed. The data in Figure 2 were selected for analysis because they are the only known data obtained at conditions which approach those experienced by sorbents injected to control SO_2. Substituting the appropriate constants, eq 17 becomes

$$k = 286\exp\left(\frac{-14500 - 3820P^{-0.111}}{T}\right) \quad (\text{in km}^{-2}\ \text{s}^{-1}) \quad (18)$$

Note that, if water also contributes to the rate of sintering, eq 17 can be extended by another exponential term.

Equations 16 and 18 are coupled to eq 1, 9, 10, and 11 by the CO_2 pressure. All six equations must be solved simultaneously.

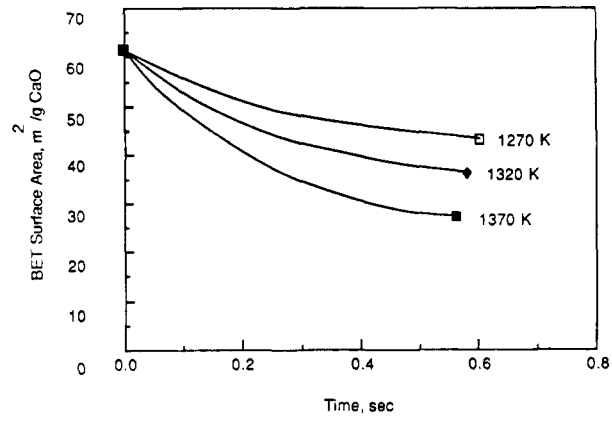

Figure 2. Isothermal flow reactor data of Borgwardt (1984) for a calcine prepared at 1270 K. The precalcine particles were conveyed by pure nitrogen. The solid lines are based on eq 16 and 18 with the parameters A and E adjusted to give the best fit.

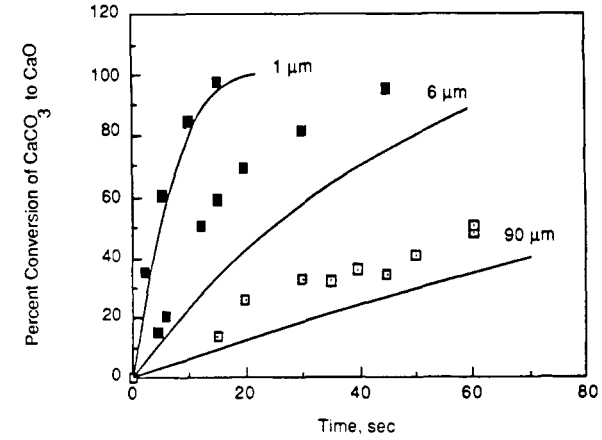

Figure 3. Calcination data of Borgwardt et al. (1986) for Georgia marble compared to model predictions showing the effect of particle size. The marble was calcined in nitrogen at 980 K in a differential reactor.

Comparisons with Data

There are two types of flow reactor data with which the model described above can be compared. One involves the use of raw carbonate or hydrate and the other involves the use of CaO of known BET surface area. In the former case, results are available which show the effects of time and temperature on surface area and extent of calcination. In the latter case, surface areas have been measured as a function of time and temperature.

The differential reactor data of Borgwardt (1985) are compared to model predictions (solid lines) in Figure 3. Percent conversion of $CaCO_3$ to CaO as a function of time

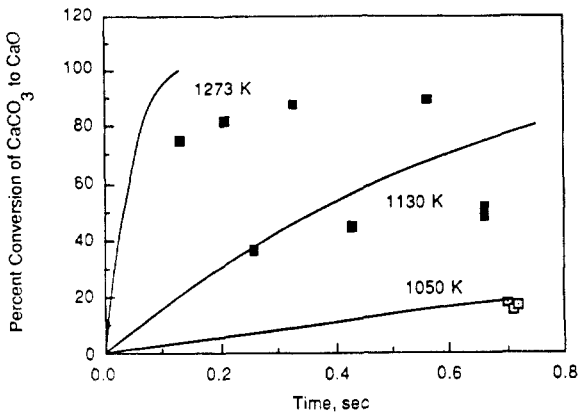

Figure 4. Data of Borgwardt (1985) for 10-μm Fredonia limestone calcined in nitrogen in a flow reactor. The solid lines are model predictions.

is shown for three particle diameters. As particle size decreases, the rate of calcination increases. This comparison tests only the chemical reaction portion of the model. Diffusion and surface area loss have little or no impact on these calculations. Note that the initial shrinking core radius is estimated from the BET surface area of the raw stone and that this core radius, rather than the particle radius, is the parameter which is changed to give the three curves in Figure 3. The relationship

$$r = \frac{3}{\rho S} \tag{19}$$

provides the necessary link between S and r.

Additional calcination results of Borgwardt, obtained in an isothermal flow reactor, are compared to predictions in Figure 4. The percent conversion of $CaCO_3$ to CaO as a function of time was obtained at three temperatures. The rate of calcination increases with increasing temperature. At all temperatures, there is a tendency for the model to overpredict the rate of reaction. The data imply that it becomes more difficult to calcine the stone as calcination proceeds. It is conceivable that this effect is due to the chemisorption of CO_2 on CaO surfaces or that the calcined material is being recarbonated in the flow reactor's sampling system. Problems of recarbonation do not occur with differential reactors, and comparison with Figure 3 shows that for differential data the model tends to underpredict the rate of calcination.

The effect of calcination temperature on CaO surface area is demonstrated by the data of Slaughter et al. (1988) in Figure 5. A high-purity, calcitic limestone, Vicron 45-3, was used in the studies. Vicron 45-3 ranges in size from 3 to 45 μm with a mean size of 11 μm. The $CaCO_3$ was calcined for 0.5 s at isothermal conditions. The data show that an optimum temperature exists for maximum surface area. The solid lines are model predictions and are based on an initial surface area for CaO of 100 m^2/g and on an asymptotic value of 5 m^2/g. These initial and final values are used in all subsequent surface area calculations. The solid lines in Figure 5 are predictions based on $CaCO_3$ particle sizes of 1, 11, and 50 μm. The 11-μm line roughly agrees with the trends seen in the data.

Figure 6 shows the effect of time on surface area development. The isothermal, flow reactor data of Slaughter et al. (1988) show surface area attaining a maximum value of 20 m^2/g at 0.32 s for the same limestone used above, Vicron 45-3, and at a temperature of 1260 K. The solid lines are predictions for diameters ranging from 1 to 50 μm. For a 5-μm particle, the predictions agree qualitatively with the observed trends, i.e., the surface area rises to a

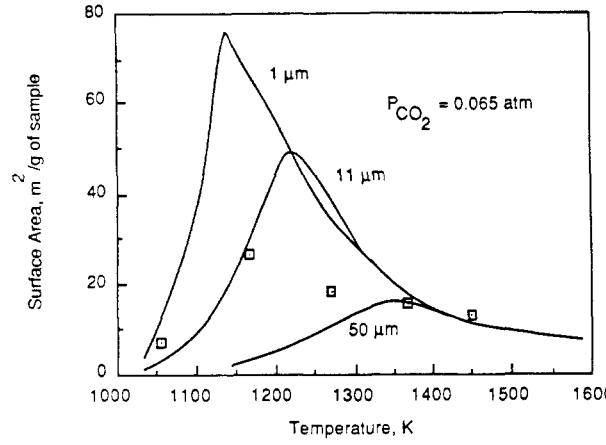

Figure 5. BET surface area data of Slaughter et al. (1988) obtained in a natural gas-burning, flow reactor at isothermal conditions and a residence time of 0.5 s. The solid lines are model predictions at particle diameters of 1, 11, and 50 μm.

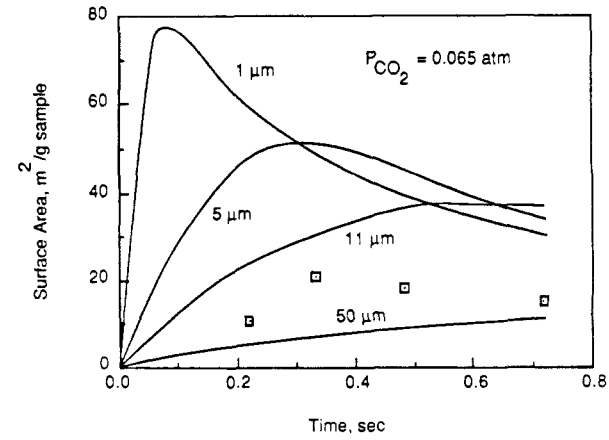

Figure 6. Data of Slaughter et al. (1988) showing the effect of time on surface area for Vicron 45-3 at an isothermal temperature of 1260 K. The solid lines are model predictions for several particle diameters.

maximum at about 0.3 s and then decreases. The predictions illustrate the advantages of using smaller limestone particles. Small $CaCO_3$ particles develop much higher surface areas in shorter times than do large particles. This is a consequence of their more rapid calcination, producing CaO which has not had time to sinter and lose surface area. Because $Ca(OH)_2$ calcines much more rapidly than $CaCO_3$, one would expect a hydrate to behave like a very small carbonate particle and achieve high surface area in a short time. The rate of hydrate decomposition, relative to that of carbonate, can be estimated from the data of Bortz and Flament (1985). The hydrate appears to decompose 50 times faster than the carbonate. The resulting predictions of surface area development for a 1-μm hydrate particle and a 5-μm carbonate particle are shown in Figure 7. The hydrate achieves its full surface area potential of 100 m^2/g in less than 1 ms. Diameters of 1 and 5 μm were selected because they roughly correspond to the sizes of the pulverized $CaCO_3$ and $Ca(OH)_2$ used to control SO_2 emissions. The CaO derived from $Ca(OH)_2$ and from $CaCO_3$ are assumed to sinter with the same kinetics.

The effect of sintering time and temperature on the surface area of a precalcined, 10-μm limestone with an initial surface area of 32 m^2/g is shown in Figure 8. The data were obtained by Cole et al. (1986) in an isothermal flow reactor fired with natural gas and show that increased temperature lowers the CaO surface area. The results also

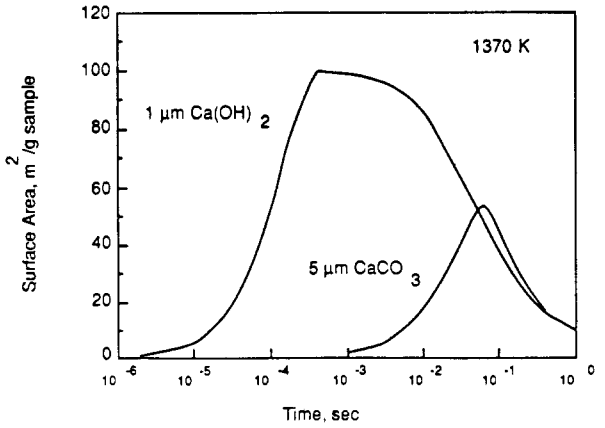

Figure 7. Model predictions comparing the rates of surface area development for carbonates and hydrates with diameters 5 and 1 μm, respectively.

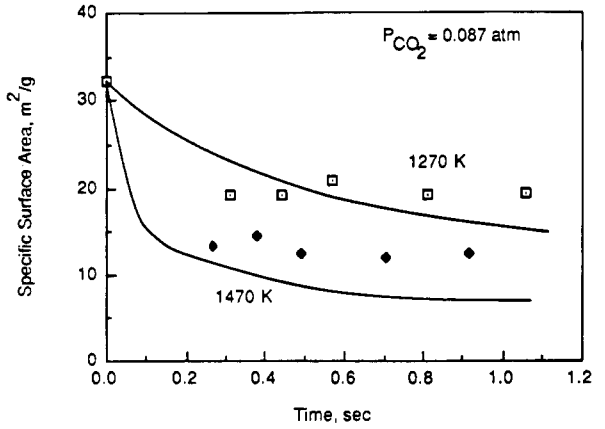

Figure 8. Isothermal, flow-reactor data of Cole et al. (1986) showing the effect of time on surface area for a 10-μm, precalcined limestone. The solid lines are model predictions.

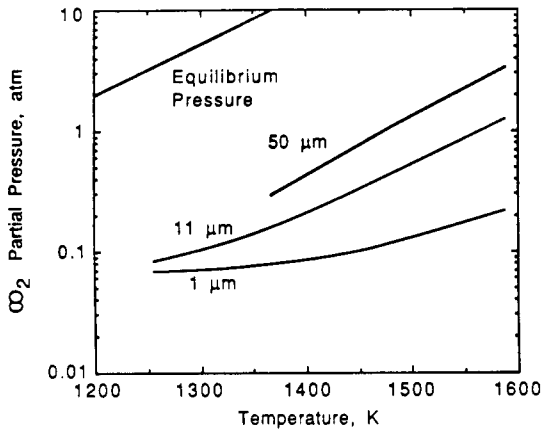

Figure 9. Model predictions of peak CO_2 partial pressures at the $CaO–CaCO_3$ interface for calcination at isothermal conditions with a bulk gas CO_2 pressure of 0.065 atm.

suggest that the CaO rapidly loses its initial surface area and that little sintering occurs after about 0.2 s. The solid lines in Figure 8 are model predictions based on the measured initial surface area of 32 m^2/g and on an asymptotic value of 5 m^2/g.

Detailed Model Predictions

The model was used to predict maximum CO_2 pressures at the $CaO–CaCO_3$ interface and to examine surface area and CO_2 profiles in calcining carbonate particles. The calculations assume an initial BET surface area of 100 m^2/g and an asymptotic value of 5 m^2/g.

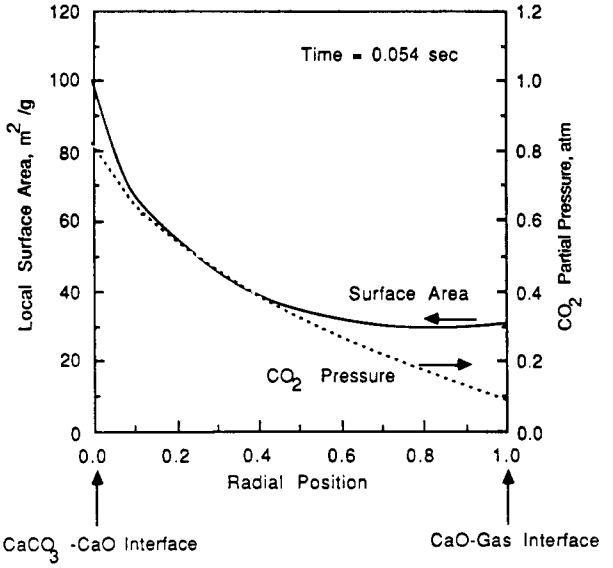

Figure 10. Model predictions showing CO_2 pressure gradients and the surface area profile for a 50-μm particle being calcined at 1480 K. The extent of calcination is 50%, and the bulk gas CO_2 pressure is 0.065 atm.

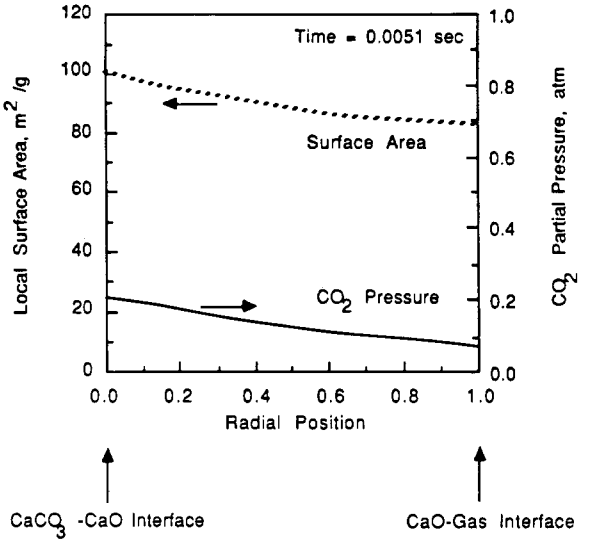

Figure 11. Model predictions showing CO_2 pressure gradients and the surface area profile for a 5-μm particle being calcined at 1480 K. The extent of calcination is 48%, and the bulk gas CO_2 pressure is 0.065 atm.

Figure 9 shows peak CO_2 partial pressures as a function of calcination temperature for particle diameters ranging from 1 to 50 μm. Peak pressures increase with increasing particle size and temperature. The dashed line in the figure indicates the equilibrium dissociation pressure of $CaCO_3$. At the highest temperature of 1600 K and for a 50-μm particle, the peak pressure was roughly 3 atm, which is well below the equilibrium value. It does not appear that the calcination process is impeded by equilibrium constraints at conditions of practical interest.

Surface area and CO_2 profiles are shown in Figure 10 for a 50-μm particle at 1478 K and Figure 11 for a 5-μm particle at the same temperature. Both figures show instantaneous profiles for particles which are 50% calcined. The 50-μm case shows steep surface area and CO_2 gradients relative to the 5-μm particle. The steep gradients are due to the 50-μm particle's size which not only offers a larger resistance to the diffusion of CO_2 but also requires a longer time to reach 50% calcination. It is the latter time factor which explains the steep surface area profile in the

50-μm particle: in the larger particle, CaO exists longer and sinters more extensively. The calculations again show the advantage of using smaller particles if calcination and sulfation are occurring simultaneously.

Conclusions

Calcination is a complex process which includes a decomposition step, diffusion of CO_2 or H_2O through porous CaO, and continuous surface area loss for all calcined material. The details of the decomposition and sintering steps are not well understood. However, the rate of the decomposition step for small, dispersed particles of $CaCO_3$ has been determined by Borgwardt (1985). Estimates of sintering rates are obtainable from the results of Borgwardt et al. (1986). The diffusion coefficients for CO_2 or H_2O in porous CaO can be estimated from theory and the results of Campbell et al. (1970). Hence, a semiempirical model of the complete calcination process is possible and was developed.

The model permits a detailed analysis of the calcination process and provides insight into the importance of physical and chemical differences between sorbents. Several important conclusions follow from the modeling:

The trends seen in calcination and CaO data can be explained within the framework of the model.

Small $CaCO_3$ particles (1 μm) yield high surface area CaO in very short times relative to larger particles (10 μm).

Smaller $CaCO_3$ particles achieve their peak surface areas at lower temperatures than do larger particles. Predicted optimum isothermal calcination temperatures for 1- and 5/-μm particles are 1144 and 1367 K, respectively, corresponding to surface areas of 75 and 20 m^2/g. Hydrates behave as extremely small carbonate particles due to their rapid rate of calcination.

Peak CO_2 pressures at the CaO–$CaCO_3$ interface are considerably below the equilibrium pressure of CO_2 at temperatures of interest. Hence, the escape of CO_2 should not significantly slow the reaction rate. The small size of hydrate particles (1–5 μm) prevents significant H_2O pressures from developing.

The practical importance of these conclusions to controlling SO_2 emissions by the direct injection of pulverized, calcium-based sorbents can be summarized briefly as follows. Smaller $CaCO_3$ particles produce more reactive CaO particles in shorter times and at lower temperatures. Hydrate particles produce more reactive CaO than do carbonates due to their small size and rapid rate of calcination.

Acknowledgment

Financial support for this work was provided by the United States Department of Energy (Contract DE-AC22-84PC70771) and the Advanced Combustion Engineering Research Center. Funds for this center are received from the National Science Foundation, the State of Utah, 25 industrial participants, and the US Department of Energy.

Nomenclature

D = diffusion coefficient of CO_2 in pore, $m^2\ s^{-1}$
D_{AB} = ordinary diffusion coefficient for CO_2 in air, $m^2\ s^{-1}$
D_{eff} = effective diffusivity of CO_2 in porous lime, $m^2\ s^{-1}$
D_K = Knudsen diffusion coefficient for CO_2, $m^2\ s^{-1}$
k = rate constant for sintering of CaO, kg $m^{-2}\ s^{-1}$
k_D = rate constant for decomposition of $CaCO_3$, kmol $m^{-2}\ s^{-1}$ atm^{-1}
k_f = mass-transfer coefficient for a sphere, m s^{-1}
M = molecular weight of $CaCO_3$, kg $kmol^{-1}$
N = number of shells of CaO plus one, also equal to the number of nodes
P = partial pressure of CO_2 at the CaO–$CaCO_3$ interface, atm
P_b = partial pressure of CO_2 in the bulk stream, atm
P_e = equilibrium dissociation pressure of CO_2, atm
P_i = partial pressure of CO_2 at node i, atm
P_t = total pressure, atm
r = radius of shrinking core of $CaCO_3$, m
R_D = decomposition rate of $CaCO_3$, kmol $m^{-2}\ s^{-1}$
R_g = gas constant = 8314.4 J $kmol^{-1}\ K^{-1}$
R_i = radial distance to node i, m
r_o = radius of particle (constant), m
S = nitrogen BET surface area, $m^2\ kg^{-1}$
T = absolute temperature, K
t = time, s

Greek Symbols

ϵ = porosity of the calcine (0.5)
ρ = density of $CaCO_3$, kg m^{-3}

Subscript

i = designation for node i where 1 is the node at the outside of the particle and N is the innermost node

Registry No. $CaCO_3$, 471-34-1; $Ca(OH)_2$, 1305-62-0; CO_2, 124-38-9; CaO, 1305-78-8; H_2O, 7732-18-5.

Literature Cited

Anderson, P. J.; Morgan, P. L. Effects of Water Vapor on Sintering of MgO. *Trans. Faraday Soc.* **1964**, *60*, 930–937.
Anderson, P. J.; Horlock, R. F.; Avery, R. G. Some Effects of Water Vapor During the Preparation and Calcination of Oxide Powders. *Proc. Br. Caram. Soc.* **1965**, *3*, 33–42.
Beruto, D.; Searcy, A. W. Calcium Oxides of High Reactivity. *Nature (London)* **1976**, *263*, 221–222.
Borgwardt, R. H. Private Communication, 1984.
Borgwardt, R. H. Calcination Kinetics and Surface Area of Dispersed Limestone Particles. *AIChE J.* **1985**, *31*, 103–111.
Borgwardt, R. H.; Roache, N. F.; Bruce, K. R. Method for Variation of Grain Size in Studies of Gas–Solid Reactions Involving CaO. *Ind. Eng. Chem. Fundam.* **1986**, *25*, 165–169.
Bortz, S.; Flament, P. Recent IFRF Fundamental and Pilot Scale Studies on the Direct Sorbent Injection Process. *Proceedings: First Joint Symp. on Dry SO_2 and Simultaneous SO_2/NO_x Control Technologies, Vol. 1*, EPA-600/9-85-020a, NTIS PB85-232353, 1985.
Campbell, F. R.; Hills, A. W. D.; Paulin, A. Transport Properties of Porous Lime and Their Influence on the Decomposition of Porous Compacts of Calcium Carbonate. *Chem. Eng. Sci.* **1970**, *25*, 929–942.
Cole, J. A.; Kramlich, J. C.; Seeker, W. R.; Silcox, G. D. Fundamental Studies of Sorbent Reactivity in Isothermal Reactors. *Proceedings: Second Joint Symposium on Dry SO_2 and Simultaneous SO_2/NO_x Control Technologies*, 1986.
Darroudi, T.; Searcy, A. W. Effect of CO_2 Pressure on the Rate of Decomposition of Calcite. *J. Phys. Chem.* **1981**, *85*, 3971–3974.
Hyatt, E. P.; Cutler, I. V.; Wadsworth, M. E. Calcium Carbonate Decomposition in Carbon Dioxide Atmosphere. *J. Am. Ceram. Soc.* **1958**, *41*, 70–74.
Luss, D. On the Pseudo Steady State Approximation for Gas Solid Reactions. *Can. J. Chem. Eng.* **1968**, *41*, 154–156.
Powell, E. K.; Searcy, A. W. Surface Areas and Morphologies of CaO Produced by Decomposition of Large $CaCO_3$ Crystals in Vacuum. *Commun. Am. Ceram. Soc.* **1982**, *March*, 42–44.
Searcy, A. W.; Beruto, D. Kinetics of Endothermic Decomposition Reactions. 2. Effects of the Solid and Gaseous Products. *J. Phys. Chem.* **1978**, *82*, 163–167.
Slaughter, D. M.; Lemieux, P. M.; Pershing, D. W.; Kirchgessner, D. Chemical and Physical Characteristics of Calcium Oxide for Enhanced SO_2 Reactivity. *AIChE J.* **1988**, in press.
Smith, J. M. *Chemical Engineering Kinetics*; McGraw-Hill: New York, New York, 1981.
Weast, R. C. *CRC Handbook of Chemistry and Physics*, 56th ed.; CRC Press: Cleveland, OH, 1975.

Received for review March 29, 1988
Revised manuscript received August 24, 1988
Accepted November 2, 1988